Published in final edited form as:
Biochemistry. 2008 August 26; 47(34): 9040–9050. doi:10.1021/bi800406w.

Concentration-Dependent Processivity of Multiple Glutamate Ligations Catalyzed by Folylpoly-γ-glutamate Synthetase

John W. Tomsho[a], **Richard G. Moran**[c], and **James K. Coward**[*,a,b]

[a]Department of Medicinal Chemistry, University of Michigan, Ann Arbor, MI 48109

[b]Department of Chemistry, University of Michigan, Ann Arbor, MI 48109

[c]Department of Pharmacology and Toxicology, Medical College of Virginia, Virginia Commonwealth University, Richmond, VA 23298

Abstract

Folylpoly-γ-glutamate synthetase (FPGS, EC 6.3.2.17) is an ATP-dependent ligase that catalyzes formation of poly-γ-glutamate derivatives of reduced folates and anti-folates such as methotrexate and 5,10-dideaza-5,6,7,8-tetrahydrofolate ($DDAH_4PteGlu_1$). While the chemical mechanism of the reaction catalyzed by FPGS is known, it is unknown whether single or multiple glutamate residues are added following each folate binding event. A very sensitive high performance liquid chromatography method has been used to analyze the multiple ligation reactions onto radiolabeled $DDAH_4PteGlu_1$ catalyzed by FPGS in order to distinguish between distributive or processive mechanisms of catalysis. Reaction time courses, substrate trapping, and pulse-chase experiments were used to measure folate release during multiple glutamate additions. Together, the results of these experiments indicate that hFPGS can catalyze the processive addition of approximately four glutamate residues onto $DDAH_4PteGlu_1$. The degree of processivity was determined to be dependent on the concentration of the folate substrate, thus suggesting a mechanism for the regulation of folate polyglutamate synthesis in cells.

Folylpoly-γ-glutamate synthetase (FPGS[1], EC 6.3.2.17) catalyzes the intracellular poly-γ-glutamylation of natural folates, such as (6*S*)-5,6,7,8-tetrahydrofolate ((6*S*)-$H_4PteGlu_1$), and antifolates, such as (6*R*)-5,10-dideaza-5,6,7,8-tetrahydrofolate ($DDAH_4PteGlu_1$, DDATHF) (Figure 1). These polyglutamylated compounds exhibit increased affinity for the target enzymes and enhanced intracellular retention (1-4). $DDAH_4PteGlu_1$ has been evaluated in clinical trials under the trade name Lometrexol as a cancer chemotherapeutic agent (5-8) while a closely related compound, pemetrexed (Alimta), is now approved for the treatment of several cancers (9). The mechanism of action of $DDAH_4PteGlu_1$ as an antitumor agent involves inhibition of glycinamide ribonucleotide formyltransferase (GARFT, EC 2.1.2.1), an essential enzyme in the *de novo* purine biosynthetic pathway (10).

FPGS has been found to convert $DDAH_4PteGlu_1$ rapidly to polyglutamate forms in cell-free reactions (11), in cells (12), and in the mouse (13). Thus, the polyglutamate forms of $DDAH_4PteGlu_1$ predominate within the cell and account for the cytotoxic action of the drug. Indeed, the hexaglutamate ($DDAH_4PteGlu_6$) metabolite has 10-fold lower K_D for GARFT than does the parent compound (14). Also, a decrease in polyglutamylation of $DDAH_4PteGlu_1$ has led to resistance due to decreased cytotoxic effects in cancer cells (12,15-17). Thus, the

[*]Author to whom correspondence should be addressed: University of Michigan, 3813 Chemistry, 930 N. University, Ann Arbor, MI 48109-1055. Phone: 734-936-2843. FAX: 734-647-4865. jkcoward@umich.edu

mechanism of FPGS-catalyzed ligation of multiple moles of glutamate to $DDAH_4PteGlu_1$ is central to our understanding of the action of $DDAH_4PteGlu_1$ and related drugs *in vivo*.

The chemical reaction catalyzed by FPGS involves simple amide bond formation via a γ-glutamyl phosphate intermediate (18). However, the reaction requires three substrates, a folate or antifolate, ATP, and glutamate, and produces three products, a γ-glutamyl peptide metabolite of the folate or antifolate, ADP, and inorganic phosphate (P_i). Investigation of this reaction is further complicated by the fact that the folate products of this reaction can generally act again as FPGS substrates. This has been shown to be the case as FPGS alone is capable of catalyzing formation of the entire range of folylpoly-γ-glutamates found in cells (11-13,19,20). Since FPGS is able to further utilize the folate products of its reaction as substrates, it may be considered a polymerase which repeatedly adds a glutamate monomer onto the growing folylpoly-γ-glutamate oligomer. An important kinetic property of polymerases is the degree of processivity of the reaction (21,22) as defined by the number of monomer additions, or turnovers, catalyzed per folate substrate binding event. Most relevant to the current study are non-template polymerization reactions such as those involved in the biosynthesis of oligosaccharides. For example, a peptidoglycan glycosyltransferase has been found to synthesize a 40-mer peptidoglycan polymer without the aid of an existing template via a processive mechanism (23,24).

Previous studies of the FPGS-catalyzed reaction involved determination of the steady-state kinetic mechanism. An Ordered Ter Ter mechanism was determined for the reaction catalyzed by FPGS isolated from three different sources utilizing different folate or antifolate substrates to which only a single glutamate was added (25-27). In all cases, the substrates bind in the order of ATP, folate/antifolate, and glutamate and the products are released in the order of ADP, folate/antifolate-Glu, and P_i (Figure 2A). If this kinetic mechanism were to hold for substrates that are converted to polyglutamates, a processive reaction, in which the ligation product remains bound while both ADP and P_i are released, would be precluded. The ligation product would also need to remain bound during the binding of another molecule each of ATP and glutamate in preparation for the next turnover (e.g., Figure 2B). $DDAH_4PteGlu_1$, like the naturally occurring tetrahydrofolates, is rapidly converted to $DDAH_4PteGlu_{5\text{-}6}$ in human

[1]Abbreviations:

5,10-CH_2-H_4PteGlu$_1$	5,10-methylene-5,6,7,8-tetrahydropteroyl glutamic acid
$DDAH_4PteGlu_1$	(6*R*)-5,10-dideaza-5,6,7,8-tetrahydropteroyl glutamic acid
$DDAH_4PteGlu_n$	(6*R*)-5,10-dideaza-5,6,7,8-tetrahydropteroyl poly-γ-glutamic acid (n = 2-6)
BSA	bovine serum albumin
DTT	dithiothreitol
FPGS	folylpoly-γ-glutamate synthetase (EC 6.2.3.17)
GARFT	glycinamide ribonucleotide formyltransferase (EC 2.1.2.1)
hFPGS	human folylpoly-γ-glutamate synthetase
HPLC	high performance liquid chromatography
$H_4PteGlu_1$	5,6,7,8-tetrahydropteroyl glutamic acid with 6*RS* stereochemistry unless otherwise specified
PAGE	polyacrylamide gel electrophoresis
TBAP	tetrabutylammonium phosphate
TCA	trichloroacetic acid
t_r	retention time

cancer cells (12), murine liver (13), and with purified recombinant human cytosolic FPGS (11) with little accumulation of short chain polyglutamates. This evidence is suggestive of a processive mechanism for human FPGS, which is investigated in the current studies.

The possibility of processivity in the reaction catalyzed by hFPGS was studied directly. $DDAH_4PteGlu_1$ was chosen as the folate acceptor substrate for several reasons. Isotopically labeled $DDAH_4PteGlu_1$ and the unlabeled polyglutamates are available via a convenient synthetic route (28), these compounds display excellent chemical stability (e.g., redox and light), and $DDAH_4PteGlu_1$ is efficiently converted to longer chain polyglutamates. In addition, determination of the steady-state kinetics of hFPGS-catalyzed glutamate ligation for each of several $DDAH_4PteGlu$ poly-γ-glutamates with hFPGS has recently been achieved (28) providing the necessary foundation for investigating the two mechanistic possibilities. In the previous work, modeling studies that assumed a strictly distributive mechanism were unable to adequately reproduce the observed pattern of substrate consumption and product distribution when $[DDAH_4PteGlu_1] \leq 10\ K_M$ (28). However, the work also indicated that at very high $DDAH_4PteGlu_1$ concentrations, 250 μM (~100 K_M), a processive mechanism was not operative as only the $DDAH_4PteGlu_2$ product was observed (28). The choice of $DDAH_4PteGlu_1$ and hFPGS provides data on an important enzyme mechanism question in the context of a clinically important enzyme-substrate pair. In this paper, we report the results of a detailed kinetics investigation of the reaction catalyzed by hFPGS including 1) a time course study monitoring the formation of all polyglutamate products and subsequent kinetic analysis, 2) substrate trapping experiments to address the validity of the reported kinetic mechanism, and 3) pulse-chase experiments (29,30) to probe directly a possible processive mechanism of FPGS-catalyzed multiple ligations.

EXPERIMENTAL PROCEDURES

Materials

Common solvents and reagents were obtained from commercial sources and were of the highest purity available. $DDAH_4PteGlu_1$, $DDAH_4Pte[^{14}C]Glu_1$, and $DDAH_4PteGlu_n$, (n = 2-6) were prepared as described previously (28). Each $DDAH_4PteGlu_n$ (n = 1-6) was dissolved in 1-2 mL of 20-100 mM NaOH.[2] The resulting solutions were clarified by filtration with a spin-filter. All solutions were then stored at −20 °C. Solution concentrations were determined based on absorbance at 272 nm (0.1 M NaOH, ε = 11,700 $M^{-1}\ cm^{-1}$) (31). Spin-X HPLC 0.2 μm nylon microcentrifuge filters (spin filters) were obtained from Costar. Partially purified hFPGS, expressed in *E. coli* or baculovirus-infected SF9 insect cells (11,32) and partially purified as described previously (33), was a generous gift of Dr. John J. McGuire. Homogenous hFPGS was expressed in baculovirus-infected SF9 insect cells and purified as described previously (11). hFPGS concentration was determined by the method of Bradford (34) and corrected for protein purity, if necessary, based on quantitative PAGE.

General Procedures

Scintillation counting used either Bio-Safe II (Research Products Inc.) or Ultima Gold (Perkin Elmer Life Sciences) scintillation cocktail. The HPLC system consisted of an auto-sampler, two pumps, a photo diode array detector, a fraction collector controlled by Varian Star v6.3 software, and was run at ambient temperature. All kinetics data were fitted using KaleidaGraph v3.5, Synergy Software (Reading, PA). Dynafit v3.28.046, BioKin Ltd. (Pullman, WA) (35) was used for kinetics modeling.

[2]γ-glutamyl peptide bond lability precludes extended storage of these compounds in solutions containing [NaOH] > 20 mM.

High Performance Liquid Chromatography (HPLC)

The conditions for ion-paired HPLC were as follows: Eluant A −100% ddH_2O. Eluant B −65% CH_3CN, 35% ddH_2O. Both eluants A and B contain 1 mM KH_2PO_4, 5 mM tetrabutylammonium phosphate (TBAP), 7 mM NaCl, and 3 mM NaN_3. Column - Vydac 218TP54, 5 μm, C18, 4.6 × 250 mm. Flow rate - 1.0 mL/min. Gradient – 0 min, 10% B; 5 min, 10% B; 10 min, 36% B; 20 min, 40% B; 50 min, 55% B; 53 min, 100% B, 58 min, 100% B. The effluent was monitored at 280 nm or by the determination of radioactivity in each fraction by liquid scintillation counting. Fractions (30 sec, 0.5 mL) for radiation chromatograms were collected directly in 5.5 mL polypropylene multi-vials for t_r = 10-60 min. Representative radiation chromatograms are shown in Figure 3 with panel A consisting solely of $DDAH_4Pte[^{14}C]Glu_1$ and panel B of a mixture of biosynthetic $DDAH_4Pte[^{14}C]Glu_n$. For analysis of reaction products, eight fractions (3-4 min, 3-4 mL) were collected corresponding to $DDAH_4PteGlu_n$ (n = 1-6) and a background (BGD). Fractions for n = 1 (two fractions, 14-18 min and 18-21 min), n = 2 (21-25 min), n = 3 (28-32 min), n = 4 (35-39 min), n = 5 (41.5-45.5 min), n = 6 (46.5-49.5 min), and a background (55-59 min) were collected directly into 20 mL glass scintillation vials. The times used to delimit the fractions were determined immediately prior to each set of HPLC analyses by injection of a mixture of biosynthetic $DDAH_4Pte[^{14}C]Glu_n$.

Liquid Scintillation Counting

Bio-Safe II scintillation cocktail (4.0 mL) was added to each fraction collected for the radiation chromatogram. Each vial was analyzed for two min to determine the DPM values. Ultima Gold scintillation cocktail (10.0 mL or 13.3 mL of cocktail for 3 mL or 4 mL of sample, respectively) was added to the fractions collected for reaction product analysis. Each vial was analyzed for two cycles of five min each to determine the DPM values.

Quantitative Analysis of Product Formation

The number of moles of the substrate and each of the polyglutamate products was determined by fractionating the eluant from a HPLC column corresponding to the position of authentic standards. The radioactivity measurements were corrected for background and the total radioactivity corrected for recovery from the column. The corrected DPM values were then converted to moles using the known specific activity of the $DDAH_4Pte[^{14}C]Glu_1$, yielding the moles of each species of $DDAH_4PteGlu_{1-6}$ present.

Determination of reaction time course

For these experiments, the following conditions were employed: 100 mM Tris (pH 8.85), 20 mM $MgCl_2$, 20 mM KCl, 10 mM $NaHCO_3$, 100 mM 2-mercaptoethanol, 0.5 mg/mL bovine serum albumin (BSA), 10 mM ATP, 5 mM glutamate, 14 nM partially purified hFPGS, and 2.5 or 25 μM $DDAH_4Pte[^{14}C]Glu_1$ (specific activity of 120.1 or 24.0 Ci/mole respectively) in a total volume of 880 μL. All reactions were assayed at 37 °C. The assay solution, lacking hFPGS, was preincubated at 37 °C for 5 min. The reactions were then initiated by the addition of ice-cold hFPGS with gentle mixing. After the desired reaction time had elapsed, an 80 μL aliquot was immediately transferred to a microcentrifuge tube and the reaction was stopped by immersion in a boiling water bath for four min. For t = 0, the aliquot was heated in a boiling water bath for two min prior to the addition of an appropriate amount of the enzyme solution after which it was immediately returned to the boiling water bath for an additional two min. The tubes were then chilled on ice. The solutions were clarified by centrifugation (8,000*g*, 10 min). The supernatant was transferred to a spin filter and filtered by centrifugation (2,000*g*, 2 min). The tube was rinsed three times with 250 μL of ddH_2O, and the rinses were then filtered as above. The filter membranes were found to retain only very low levels of radioactivity. The filtered solutions were evaporated at ambient temperature overnight on a vacuum centrifuge,

the resulting residues were reconstituted with 80 μL ddH_2O, and stored at −80 °C pending analysis by ion-pair HPLC.

Calculation of the concentration of hFPGS·$DDAH_4PteGlu_1$ (E·S) complex

[ES] was determined based on the total hFPGS concentration, $[E]_t$, $DDAH_4PteGlu_1$ concentration, [S], and the K_M value for $DDAH_4PteGlu_1$(Eq. 1) (36).

$$[ES] = \frac{[E]_t * [S]}{K_M + [S]} \quad (1)$$

Substrate trapping experiments (Supporting Information, Figure S2)

For these experiments, the following conditions were employed: 100 mM Tris (pH 8.80), 10 mM $MgCl_2$, 20 mM KCl, 10 mM $NaHCO_3$, 5 mM DTT, 0.5 mg/mL BSA, 10 mM ATP, 5 mM glutamate, 25 μM $DDAH_4PteGlu_1$ (preincubation and trapping solutions), and 105 nM homogeneous hFPGS in a final volume of 80 μL. All reactions were assayed in triplicate at 37 °C and stopped by the addition of TCA (50% w/v to a final concentration of 5% w/v). A preincubation solution was prepared that lacked ATP, glutamate, and hFPGS, but contained high (249 Ci/mole) or low (24.9 Ci/mole) specific activity $DDAH_4Pte[^{14}C]Glu_1$ for the substrate trapping and control experiments, respectively. A trapping solution was prepared that lacked only hFPGS, but contained ATP, glutamate, and either unlabeled $DDAH_4PteGlu_1$ or low specific activity $DDAH_4Pte[^{14}C]Glu_1$ for the trapping and control experiments, respectively. Both the preincubation and trapping solutions were incubated at 37 °C for 5 min. hFPGS was then added to the preincubation solution yielding an enzyme concentration of 1.05 μM. After an additional 5 min at 37 °C, the reaction was initiated by the addition of the trapping solution to a preincubation solution containing hFPGS, resulting in a 10-fold dilution of FPGS. After the desired reaction time had elapsed, the reaction was stopped by addition of TCA (50% w/v to a final concentration of 5% w/v). To obtain a t = 0 min data point, TCA was added to the hFPGS-containing preincubation solution prior to the addition of the trapping solution. Following the TCA quench, reactions were chilled on ice. The reaction solutions were then clarified by centrifugation (16,000*g*, 10 min) and stored at −80 °C pending analysis by ion-pair HPLC.

Pulse-chase experiments. (Supporting Information, Figure S4)

For experiments where $[DDAH_4PteGlu_1]$ = 25 μM during the chase phase, the following conditions were employed: 100 mM Tris (pH 8.80), 10 mM $MgCl_2$, 20 mM KCl, 10 mM $NaHCO_3$, 5 mM DTT, 0.5 mg/mL BSA, 10 mM ATP, 5 mM glutamate, 25 μM $DDAH_4PteGlu_1$ (pulse and chase phases), and 1.0 μM homogeneous hFPGS in a final volume of 80 μL. All reactions were assayed in triplicate at 37 °C and stopped by the addition of TCA (50% w/v to a final concentration of 5% w/v). A pulse solution was prepared that lacked only hFPGS, but contained high specific activity $DDAH_4Pte[^{14}C]Glu_1$ (249 Ci/mole). A chase solution was prepared with unlabeled $DDAH_4PteGlu_1$. Both the pulse and chase solutions were preincubated at 37 °C for 5 min. To obtain the t = 0 min data points, TCA was added to the preincubated pulse solution followed by hFPGS, to 10 μM, and finally chase solution. For the t = 2 min pulse data points, the reaction was initiated by addition of hFPGS to 10 μM in the pulse solution. TCA was then added at t = 2 min to stop the reaction prior to the addition of chase solution. To obtain the chase data points, the reaction was initiated as above and the chase solution was added at t = 2 min. The reaction was stopped at the desired time by removing an aliquot from the common reaction solution and adding it to a tube containing TCA. In all cases, addition of the chase solution resulted in a *ca*. 10-fold dilution of FPGS. For all points,

the tubes containing the quenched reactions were immediately placed on ice, then clarified by centrifugation (16,000*g*, 10 min), and stored at −80 °C pending analysis by ion-pair HPLC.

For experiments where [$DDAH_4PteGlu_1$] = 250 μM during the chase phase, the conditions were as described directly above, with the following exceptions. hFPGS was added to the pulse solution such that the concentration was 1.02 μM. $DDAH_4PteGlu_1$ was 25 μM in the pulse phase and 250 μM in the chase phase. The chase solution consisted of 9.01 mM unlabeled $DDAH_4PteGlu_1$. 1.0 μM was the final concentration of homogeneous hFPGS.

RESULTS AND DISCUSSION

Steady-state kinetics data obtained previously at a single time point (28) provided the basis for the more extensive time course experiments described herein. Investigation of possible processivity in the reaction catalyzed by hFPGS was initiated by determination of the time course (0 – 120 min) of the reaction utilizing $DDAH_4Pte[^{14}C]Glu_1$ at two different concentrations, 2.5 μM (~ K_M,Figure 4A) and 25 μM (~ 10 K_M,Figure 4B). These data clearly show that the degree of multiple glutamate ligations to $DDAH_4PteGlu_1$ is concentration-dependent. The results of this experiment are very similar to those observed for partially purified rat liver FPGS with $H_4PteGlu_1$ as the substrate (20); multiple glutamate ligations to $H_4PteGlu_1$ at low concentrations (5 μM, ~K_M) yielded $H_4PteGlu_{4\text{-}5}$ as the predominant products following initial formation and consumption of $H_4PteGlu_2$ and $H_4PteGlu_3$. In contrast, $H_4PteGlu_1$ at a higher concentration (35 μM, ~10 K_M) yielded predominately $H_4PteGlu_2$ and $H_4PteGlu_3$ as the initial products, but lower relative amounts of $H_4PteGlu_{4\text{-}5}$ products were observed at longer reaction times. The time course data for the reaction containing 2.5 μM $DDAH_4Pte[^{14}C]Glu_1$ (Figure 4A) agree well with what was observed in whole CCRF-CEM cells (12) and in the livers of mice (13) that were treated with $DDAH_4PteGlu_1$, thus providing a strong correlation between data obtained in cell-free experiments and those obtained in intact cells or *in vivo*.

These data (Figure 4) are strongly suggestive of a processive reaction. When considered together with a simplified kinetic scheme (Figure 5), the time course data for 2.5 μM $DDAH_4PteGlu_1$ (Figure 4A) indicate that the rates of glutamate ligation, $k_2[E{\cdot}S_2]$, $k_3[E{\cdot}S_3]$, and $k_4[E{\cdot}S_4]$, are much greater than the corresponding rates of dissociation, $k_6[E{\cdot}S_2]$, $k_7[E{\cdot}S_3]$, and $k_8[E{\cdot}S_4]$. Since the $DDAH_4PteGlu_5$ product (S_5) accumulates in this reaction, the rate of dissociation, $k_9[E{\cdot}S_5]$, is greater than the rate of further ligation, $k_5[E{\cdot}S_5]$. However, the rate, $k_5[E{\cdot}S_5]$, is apparently not zero because small amounts of the $DDAH_4PteGlu_6$ product (S_6) are observed at longer reaction times (Figure 4A). Similarly, inspection of the 25 μM $DDAH_4PteGlu_1$ time course data (Figure 4B) shows continued accumulation of the triglutamate, $DDAH_4PteGlu_3$ (S_3), in the presence of a large amount of the monoglutamate, $DDAH_4PteGlu_1$ (S_1). This demonstrates that the rate of ligation, $k_2[E{\cdot}S_2]$, is greater than dissociation, $k_6[E{\cdot}S_2]$. The fact that tetra- and pentaglutamates, $DDAH_4PteGlu_4$ (S_4) and $DDAH_4PteGlu_5$ (S_5), are detected at longer times indicates that the ligation rates $k_3[E{\cdot}S_3]$ and $k_4[E{\cdot}S_4]$ can ultimately prevail over the dissociation rates, $k_7[E{\cdot}S_3]$ and $k_8[E{\cdot}S_4]$. This behavior is also consistent with a processive mechanism. Finally, the time course data shown in Figure 4 were subjected to a kinetics modeling analysis using DynaFit (v.3.28.046). Nine variants of the scheme shown in Figure 5 were evaluated (Supporting Information, Figure S1), each of which allow for either processive or distributive modes of multiple glutamate additions. Although excellent visual fits to the experimental data were obtained, error analysis of the rate constants derived from the fits led mainly to large uncertainties in the modeled rate constants. Similarly, values for the processivity factors, $P = k_{cat}/(k_{cat} + k_{off})$, could not be obtained with certainty by this analysis.

In order to assess directly a possible processive kinetic mechanism in the reaction catalyzed by FPGS, substrate trapping and pulse-chase experiments were pursued. A substrate trapping experiment was performed to assess the formation of a catalytically competent binary complex, hFPGS·$DDAH_4Pte[^{14}C]Glu_1$ ("E-Folate", Figure 2B). An experiment which results in increased incorporation of $DDAH_4Pte[^{14}C]Glu_1$, into polyglutamates due to substrate trapping would indicate that the binary complex forms and is catalytically competent. Failure to observe substrate trapping would be consistent with one of three scenarios: 1) the binary complex does not form, 2) it does form but is rapidly exchanged with free substrate, or 3) it does form but is not catalytically competent. The substrate trapping experiment addresses directly the interpretation of the previously determined kinetic mechanism of FPGS (25-27) that precludes the kinetic competence of the hFPGS·$DDAH_4Pte[^{14}C]Glu_1$ binary complex and therefore a processive mechanism. These previous studies, however, were carried out under conditions in which the question of a processive catalytic mechanism could not be addressed. Specifically, the *Corynebacterium* FPGS produces only the $H_4PteGlu_2$ product when $H_4PteGlu$ is utilized as the substrate (25). FPGS from hog liver or *L. casei* catalyzes the ligation of glutamate to aminopterin (27) or 5,10-CH_2-$H_4PteGlu_2$ (26), respectively. However, the products derived from a single ligation reaction, aminopterin-Glu and 5,10-CH_2-$H_4PteGlu_3$, are very poor substrates for further catalysis by the respective FPGS enzymes. Therefore, in all of these previous studies, the reaction conditions, enzyme source, and substrate were chosen to prevent multiple turnovers of the folate or antifolate substrate. A substrate trapping experiment allows for a direct evaluation of the proposed Ordered Ter Ter kinetic mechanism with the enzyme-substrate pair, hFPGS·$DDAH_4Pte[^{14}C]Glu_1$, under multiple ligation conditions. The design of the substrate trapping experiments is shown in the Supporting Information, Figure S3.

Preincubation of hFPGS (105 nM) and high specific activity $DDAH_4Pte[^{14}C]Glu_1$ (25 μM) was carried out for 5 min prior to initiation of the reaction to allow the formation of the postulated E·S binary complex. The reaction was initiated by the addition of ATP and glutamate at saturating concentrations with concurrent trapping by addition of 10 volumes of 25 μM unlabeled $DDAH_4PteGlu_1$. This results in a 10-fold reduction of specific activity while maintaining constant substrate concentration. The reaction was allowed to proceed for a given time (0 – 6 min) prior to quenching by the addition of TCA to obtain a time course of the reaction. A control reaction involved the same procedure except $DDAH_4Pte[^{14}C]Glu_1$ of a low specific activity, identical to the final specific activity achieved in the substrate trapping experiment, was used in *both* the preincubation and trapping phases. If the hFPGS·$DDAH_4Pte[^{14}C]Glu_1$ binary complex forms during preincubation and is catalytically active, the reaction will proceed with the enzyme-bound, high specific activity substrate when initiated. When a polyglutamate product is released following ligation of Glu to $DDAH_4Pte[^{14}C]Glu_1$, this high specific activity product would be diluted by the large excess of unlabeled $DDAH_4PteGlu_1$. In contrast, if the hFPGS·$DDAH_4Pte[^{14}C]Glu_1$ binary complex does not form, is not catalytically competent, or exchanges rapidly with free substrate, the high specific activity substrate used in the preincubation would be immediately diluted with the unlabeled $DDAH_4PteGlu_1$, yielding a pool of low specific activity substrate that would then be available to FPGS for reaction. This scenario would result in the formation of polyglutamate products of low specific activity, equivalent to the control reaction, whether or not the hFPGS·$DDAH_4Pte[^{14}C]Glu_1$ binary complex is competent. The experiment is illustrated schematically in the Supporting Information, Figure S2.

When compared with the control experiment, there is an increase in the amount of product formed at each time point in the substrate trapping experiment (Figure 6). This indicates that the high specific activity substrate used in the substrate trapping reaction forms a hFPGS·$DDAH_4Pte[^{14}C]Glu_1$ binary complex that is kinetically competent. Extrapolation of the time course data to t = 0 min indicates that an additional 34.1 ± 5.2 pmoles of glutamate were incorporated into product in the substrate trapping experiment vs. that incorporated in the

control experiment. The concentration of hFPGS·$DDAH_4PteGlu_1$ (E·S) complex present in this experiment was calculated to be 98.5 nM (Eq 1) based on a total hFPGS concentration and $DDAH_4PteGlu_1$ concentration of 105 nM and 25 μM, respectively. Under these conditions, the K_M value for $DDAH_4PteGlu_1$ was determined to be 1.65 μM (data not shown). Considering the final reaction volume of 75 μL and [E·S] = 98.5 nM, a total of 7.39 pmoles of E·S complex was present. Therefore, an average of 4.6 ± 0.7 moles of glutamate were added per mole of hFPGS·$DDAH_4PteGlu_1$ complex formed. This result is supported by determination of the amount of $DDAH_4PteGlu_n$ products formed in the substrate trapping (Figure 7A) and control (Figure 7B) experiments, as well as the *difference* in oligo-γ-glutamate (n = 1-6) formation between the two experiments (Figure 7C) during the time period involved. These data demonstrate a much greater production of long-chain polyglutamate products (n = 3-6) under substrate trapping conditions than in the control experiment, thus confirming the conversion of enzyme-bound $DDAH_4PteGlu_1$ to long-chain products. They are consistent with the calculated stoichiometry of 4.6 moles of glutamate incorporated per mole of E·S complex, and support formation of kinetically competent hFPGS·$DDAH_4PteGlu_1$ binary complex. The only reasonable explanation for the observation that [P]:[E·S] > 1 is that the initial substrate in the binary complex undergoes multiple turnovers. These data are interpreted as direct evidence of a processive mechanism of catalysis under these conditions.

A notable feature of the substrate trapping data (Figure 6) is a non-zero y-intercept for the control reaction. Examination of product distribution data for the control reaction (Figure 7B) reveals that an apparent burst of product formation occurs primarily in the formation of $DDAH_4PteGlu_2$. Similar results were observed when a similar but more extended reaction time course (0 – 120 min) was examined, also at 25 μM $DDAH_4PteGlu_1$ (Figure 4B).

The observation of a burst in formation of $DDAH_4PteGlu_2$, the product of the first ligation, followed by a slower, steady-state ligation of additional glutamates in both the control and substrate trapping reactions (Figure 7), is also consistent with a processive mechanism. In a processive polymerization reaction, it is necessary for the product of the reaction to reorient itself in the active site prior to the next round of catalysis. For the FPGS reaction, the newly formed C-terminal glutamate of $DDAH_4PteGlu_2$, assumed to form rapidly from the substrate-based quaternary complex, hFPGS·$DDAH_4Pte[^{14}C]Glu_1$·ATP·Glu, occupies the binding site of the incoming glutamate substrate immediately following catalysis. For another round of catalysis to occur, several events need to occur: 1) the C-terminal glutamate of the polyglutamate product must be released from the incoming glutamate binding site, 2) two of the products, ADP and P_i, must be released, 3) ATP and glutamate must bind to FPGS, and 4) the C-terminal glutamate of the polyglutamate product must be repositioned such that the γ-carboxylic acid is adjacent to the γ-phosphorus of ATP (18). Together, these steps require a rearrangement of the active site and suggest a mechanism in which the chemical step of peptide bond formation is followed by a slower, rate-limiting rearrangement of the newly formed hFPGS·$DDAH_4Pte[^{14}C]Glu$-γ-Glu_n binary complex, thus giving rise to a burst. Rearrangement of the FPGS active site during catalysis was suggested previously, based on poor substrate activity of a α-descarboxy analog of methotrexate (37).

The proposed processive mechanism of hFPGS-catalyzed ligation of multiple glutamate residues to $DDAH_4PteGlu_1$ was further investigated by pulse-chase experiments.[3] The design of the pulse-chase experiment is shown in the Supporting Information, Figure S5. Experiments of this type are generally used in conjunction with kinetic isotope effect studies to determine

[3]Prior to carrying out the pulse-chase experiments, a standard control experiment checking for a reaction in the absence of added ATP and glutamate was required. hFPGS expressed in baculovirus-infected SF9 insect cells and purified to homogeneity (11) was assayed for product formation in the absence of ATP and glutamate. No product formation was detected (data not shown) thereby demonstrating that, in contrast to partially purified hFPGS (38), no ATP or glutamate was retained in the course of purifying the enzyme to homogeneity

the commitment to catalysis (39) and are conceptually related to the substrate trapping experiments described above. The major difference between pulse-chase experiments and substrate trapping experiments is that, in the former, the reaction is already proceeding with the high specific activity substrate (pulse) when the unlabeled substrate (chase) is added. The time course of the reaction after addition of the chase is determined and then extrapolated back to t_1, the time when the chase was initiated. The point at which the extrapolated line intersects t_1, the chase initiation time, is compared with a time point obtained when an identical reaction is quenched at t_1 instead of adding the chase. This experiment is illustrated schematically in the Supporting Information, Figure S4.

If the enzyme-bound, high specific activity substrate is able to exchange with free, unlabeled substrate in solution at a much faster rate than catalysis, $k_{off} \gg k_{cat}$, then the extrapolated line based on the time-dependent chase data will intersect the data point obtained by quenching the pulse at $t = t_1$, hereafter described as the "quench point." This result would indicate that a distributive mechanism is operative because catalysis is slow compared to dissociation. However, if the chase data extrapolate to a point at t_1 that is greater than the quench point, catalysis is faster than dissociation, $k_{cat} \gg k_{off}$. This would provide strong evidence for a processive mechanism. The difference between the extrapolated chase data point and the quench point at t_1 is directly proportional to the amount of enzyme-bound high specific activity substrate that is converted to product.

Two pulse-chase experiments were performed, each of which involved a pulse of 25 μM $DDAH_4Pte[^{14}C]Glu_1$.[4] The first experiment utilized 25 μM $DDAH_4PteGlu_1$ as the chase (Figure 8A), while the second experiment utilized 250 μM $DDAH_4PteGlu_1$ as the chase (Figure 8B). The concentration of 25 μM $DDAH_4Pte[^{14}C]Glu_1$ (K_M = 1.65 μM, *vide supra*) in the pulse was chosen to ensure near saturation of the enzyme while maintaining the production of long-chain polyglutamate products (Figure 3B). The concentrations of $DDAH_4PteGlu_1$ present in the chase were chosen to enhance (25 μM, Figure 4B) or preclude (250 μM) (28) the formation of long-chain polyglutamates. Upon examination of the results of these experiments, it is immediately apparent that in the 25 μM chase experiment (Figure 8A) the enzyme-bound labeled substrate is converted to product after addition of the chase since the chase data extrapolate to $t = t_1$, 2 min) at a point that is greater than the quench point. This is not the case in the experiment with the 250 μM chase (Figure 8B) where the chase data extrapolate to $t = t_1$ at a point that is equal to the quench point. These data are consistent with the concentration-dependent distribution of polyglutamate products previously demonstrated (20,28).

In a detailed analysis of the experimental results, the difference between the extrapolated chase data and the quench point at t_1 observed in Figure 8A was evaluated quantitatively. Additional product formation in the amount of 540 ± 186 pmoles over that predicted from the pulse data had occurred in the 25 μM chase experiment (Figure 8A). When divided by the amount of E·S complex present (75 pmoles, Eq 1), it was determined that 7.2 ± 2.5 glutamate additions per E·S complex occurred under the conditions employed in these experiments. The experimental design of the 25 μM pulse-chase experiment involved the use of a chase in which the concentration of unlabeled $DDAH_4PteGlu_1$ was equal to that utilized in the pulse solution, 25 μM. This required the use of a volume dilution to chase the labeled $DDAH_4PteGlu_1$ originally present in the pulse and therefore a concentration of hFPGS in the pulse phase that was 10-fold greater than in the final reaction mixture. The small volume of the pulse solution (8 μL) combined with the high hFPGS concentration (10 μM) resulted in the consumption of nearly

[4]An experiment in which the final concentration of all DDATHF would be 2.5 μM, resulting from a pulse of high specific activity DDATHF (2.5 μM) followed by a chase of unlabeled DDATHF (2.5 μM), proved not to be feasible. Under such conditions where [S] is limiting, most DDATHF would be bound to FPGS leaving a large amount of free enzyme. In addition, the overall amount of product formed would be about ca. 50% of that seen for the higher concentrations of substrate, leading to a lower signal to noise ratio.

50% of the substrate present in the 25 μM pulse and may explain the larger than expected average ratio of product formation to E·S complex. In contrast, the 250 μM pulse-chase experiment (Figure 8B), utilized an approximately 10-fold lower concentration of hFPGS in the pulse phase. In this experiment, a small volume of a high concentration solution (9.01 mM) of unlabeled $DDAH_4PteGlu_1$ was added as the chase. This experimental design was predicated on the fact that the final concentration of the $DDAH_4PteGlu_1$ in the chase was 10-fold greater, 250 μM, than that used in the pulse, 25 μM. In both pulse-chase experiments, the final concentration of hFPGS was identical and the specific activity of $DDAH_4Pte[^{14}C]Glu_1$ utilized in the pulse was diluted by 10-fold during the chase phase. The only plausible explanation for an observed [P]:[E·S] > 1 is that the initial substrate in the binary complex undergoes multiple turnovers. Thus, the results of the 25 μM pulse-chase experiment are consistent with a processive mechanism. However, a distributive mechanism is indicated in the experiment that utilized 250 μM $DDAH_4PteGlu_1$ in the chase. Together, these data provide direct evidence in support of a concentration-dependent processive mechanism for FPGS-catalyzed ligation of multiple glutamate residues to $DDAH_4PteGlu_1$.

The observed concentration-dependent processivity may be the result of folate heterocycle binding at two different sites. The possibility that FPGS may possess two folate binding sites was first suggested in a computational analysis of ligand binding based on the structure of the enzyme isolated from *L. casei* (40). This analysis identified a new site that binds monoglutamates with higher affinity than the site originally identified in the crystal structure (41), which is now postulated to bind primarily polyglutamate derivatives. Mathieu et al. provided independent support of this hypothesis based on the structure of a bifunctional protein, *folC* from *E. coli*, which harbors both dihydrofolate synthetase (DHFS) and FPGS activities (42). In the *folC* work, the two binding sites were associated with the binding of two different substrates, 7,8-dihydropteroic acid (DHFS) and 5,6,7,8-tetrahydrofolic acid (FPGS), for the bifunctional enzyme. The two binding site hypothesis is also supported by recent experiments involving “domain swap” chimeric proteins and selected site-directed mutants of both *L. casei* FPGS and *folC* (43).

During processive catalysis, the $DDAH_4PteGlu_1$ substrate could bind at one of two folate binding sites and initial glutamate ligation would occur. Under conditions of low concentration of the folate substrate, the glutamate tail would remain bound while the heterocycle (i.e., pterin or analog) would migrate to the second binding site. Once the heterocycle is bound at the second site, the C-terminus of the $DDAH_4PteGlu_2$ product would rearrange to position the γ-carboxyl of the terminal glutamate in close proximity to ATP for a second glutamate ligation reaction via the acyl phosphate intermediate (18). Subsequent multiple glutamate ligation reactions would occur with the heterocycle bound at the second site which is postulated to bind preferentially the polyglutamate derivatives (40,43). A similar translocation of the electrophilic substrate, glutathione (GSH), is postulated in the reaction catalyzed by glutathionylspermidine synthetase (GspS, EC 6.3.1.8) based on crystallographic evidence; i.e., the position of GSH in the dead-end complex, GspS · GSH · ADP vs. the GSH portion of a phosphorylated bi-substrate phosphinic acid-containing pseudopeptide inhibitor (I) in the complex, GspS · I · ADP (44).

This proposed sequence of events is consistent with the observed burst in formation of the first ligation product, $DDAH_4PteGlu_2$, followed by slow steady-state ligation of additional glutamates. However at high concentration of the folate substrate, it is possible that the monoglutamate substrate could bind to both sites thus preventing the postulated rearrangement just described. Under such conditions, the initial diglutamate product would dissociate without formation of higher polyglutamates, thus resulting in the observed distributive mechanism.

CONCLUSIONS

Three experimental approaches were used to probe the degree of processivity of the reaction catalyzed by the ATP-dependent ligase, hFPGS, involving the multiple glutamylation of $DDAH_4Pte[^{14}C]Glu_1$. The formation of products of multiple turnovers in the presence of a large excess of monoglutamate substrate was observed. If the kinetic constants obtained for each polyglutamate, $DDAH_4PteGlu_n$ (n = 2-6), as a substrate (28) are taken into account, it is apparent that continued addition of glutamate is preferred to dissociation. This result is consistent with a processive mechanism. The second experiment involved a substrate trapping approach and probed directly for the formation and kinetic competence of the hFPGS·$DDAH_4PteGlu_1$ (E·S) complex. A significant commitment to catalysis (39) was observed in the substrate trapping reaction, indicating that a catalytically competent E·S complex is formed and that multiple glutamate ligation reactions occur for each initial E·S complex formed without dissociation of intermediate products. Pulse-chase experiments were then used to confirm the apparent processivity of the hFPGS-catalyzed reaction. Reaction progress data obtained during the chase phase at a low but still saturating folate substrate concentration (25 μM, ~10 K_M), extrapolated to $t = t_1$ significantly above that of the corresponding quench point. These experiments confirmed that multiple moles of glutamate were added per mole of $DDAH_4PteGlu_1$ in an E·S complex under these conditions. Additionally, it was determined that the reaction catalyzed by hFPGS is not processive at a supersaturating concentration of folate substrate (250 μM, ~100 K_M) in the chase phase, consistent with the previously observed formation of $DDAH_4PteGlu_2$ as the major reaction product (78%) at this high concentration (28).

In summary, a combination of time course, substrate trapping, and pulse-chase experiments leads to the conclusion that hFPGS catalyzes multiple ligations of glutamic acid to $DDAH_4PteGlu_1$ in a processive fashion but the degree of processivity is dependent on the concentration of the $DDAH_4PteGlu_1$ substrate. If this finding extends to the natural folates as hFPGS substrates, the concentration dependence of processivity in folylpoly-γ-glutamate biosynthesis may have evolved as a mechanism for regulation of folate homeostasis in the cell. Thus, low intracellular concentrations of folate would encourage the formation of long-chain polyglutamate metabolites thereby increasing their retention with in the cell and efficacy as cofactors. However, at high concentrations of folate, cellular retention is not required and long-chain polyglutamate metabolite formation is curtailed, thus allowing folate efflux from the cell while minimizing unnecessary consumption of ATP.

Supplementary Material

Refer to Web version on PubMed Central for supplementary material.

Acknowledgments

We are most grateful to Dr. John McGuire and Mr. Bill Haile, Roswell Park Cancer Institute, Buffalo, NY, for their gift of partially purified FPGS used in the time course experiments and initial substrate trapping experiments. We thank Prof. Bruce Palfey and Dr. Scott Nelson for assistance with the kinetic modeling studies. We also thank Prof. Carol Fierke for helpful discussions regarding experimental design and Prof. Anthony Berdis for critical comments on the manuscript.

Funding information: This research was supported in part by grants from the National Cancer Institute, CA 28097 (J.K.C.), CA 39687 (R.G.M.). J.W.T. was a trainee of the Michigan Chemistry-Biology Interface Training Program, supported in part by a grant from the National Institutes of General Medical Sciences (GM008597). J.W.T. was the recipient of a Fred W. Lyons Fellowship from the College of Pharmacy, University of Michigan, and a fellowship from the American Foundation for Pharmaceutical Education.

REFERENCES

1. McGuire JJ, Bertino JR. Enzymatic synthesis and function of folylpolyglutamates. Mol. Cell. Biochem 1981;38:19–48. [PubMed: 7027025]
2. McGuire, JJ.; Coward, JK. Pteroylpolyglutamates: Biosynthesis, degradation, and function. In: Blakley, RL.; Benkovic, SJ., editors. Folates and pterins. John Wiley & Sons; New York: 1984. p. 135-190.
3. Shane B. Folylpolyglutamate synthesis and role in the regulation of one-carbon metabolism. Vitamins and Hormones-Advances in Research and Applications 1989;45:263–335.
4. Faessel HM, Slocum HK, Jackson RC, Boritzki TJ, Rustum YM, Nair MG, Greco WR. Super *in vitro* synergy between inhibitors of dihydrofolate reductase and inhibitors of other folate-requiring enzymes: The critical role of polyglutamylation. Cancer Res 1998;58:3036–3050. [PubMed: 9679969]
5. Mendelsohn, LG.; Worzalla, JF.; Walling, JM. Preclinical and clinical evaluation of the glycinamide ribonucleotide formyltransferase inhibitors Lometrexol and LY309887. In: Jackman, AL., editor. Antifolate Drugs in Cancer Therapy. Humana; Totowa, N.J.: 1999. p. 261-280.
6. Adams J, Elliott PJ. New agents in cancer clinical trials. Oncogene 2000;19:6687–6692. [PubMed: 11426656]
7. McGuire JJ. Anticancer antifolates: Current status and future directions. Curr. Pharm. Des 2003;9:2593–2613. [PubMed: 14529544]
8. Purcell WT, Ettinger DS. Novel antifolate drugs. Current Oncology Reports 2003;5:114–125. [PubMed: 12583828]
9. Rollins KD, Lindley C. Pemetrexed: A multitargeted antifolate. Clin. Therap 2005;27:1343–1382. [PubMed: 16291410]
10. Beardsley GP, Moroson BA, Taylor EC, Moran RG. A new folate antimetabolite, 5,10-dideaza-5,6,7,8-tetrahydrofolate is a potent inhibitor of *de novo* purine synthesis. J. Biol. Chem 1989;264:328–333. [PubMed: 2909524]
11. Sanghani PC, Moran RG. Purification and characteristics of recombinant human folylpoly-gamma-glutamate synthetase expressed at high levels in insect cells. Protein Expr. Purif 2000;18:36–45. [PubMed: 10648167]
12. Pizzorno G, Sokoloski JA, Cashmore AR, Moroson BA, Cross AD, Beardsley GP. Intracellular metabolism of 5,10-dideazatetrahydrofolic acid in human leukemia cell lines. Mol. Pharmacol 1991;39:85–89. [PubMed: 1702876]
13. Habeck LL, Chay SH, Pohland RC, Worzalla JF, Shih C, Mendelsohn LG. Whole-body disposition and polyglutamate distribution of the GAR formyltransferase inhibitors LY309887 and lometrexol in mice: Effect of a low folate diet. Cancer Chemother. Pharmacol 1998;41:201–209. [PubMed: 9443636]
14. Sanghani SP, Moran RG. Tight binding of folate substrates and inhibitors to recombinant mouse glycinamide ribonucleotide formyltransferase. Biochemistry 1997;36:10506–10516. [PubMed: 9265631]
15. McGuire, JJ. Antifolate polyglutamylation in preclinical and clinical antifolate resistance. In: Jackman, AL., editor. Antifolate drugs in cancer therapy. Humana; Totowa, N.J.: 1999. p. 339-363.
16. Zhao RB, Titus S, Gao F, Moran RG, Goldman ID. Molecular analysis of murine leukemia cell lines resistant to 5,10-dideazatetrahydrofolate identifies several amino acids critical to the function of folylpolyglutamate synthetase. J. Biol. Chem 2000;275:26599–26606. [PubMed: 10856298]
17. Liani E, Rothem L, Bunni MA, Smith CA, Jansen G, Assaraf YG. Loss of folylpoly-γ-glutamate synthetase activity is a dominant mechanism of resistance to polyglutamylation-dependent novel antifolates in multiple human leukemia sublines. Int. J. Cancer 2003;103:587–599. [PubMed: 12494465]
18. Banerjee R, McGuire JJ, Shane B, Coward JK. Dihydrofolate synthetase and folylpolyglutamate synthetase: Direct evidence for intervention of acyl phosphate intermediates. Biochemistry 1988;27:9062–9070. [PubMed: 2906805]
19. McBurney MW, Whitmore GF. Isolation and biochemical characterization of folate deficient mutants of Chinese-hamster cells. Cell 1974;2:173–182. [PubMed: 4547236]

20. McGuire JJ, Hsieh P, Coward JK, Bertino JR. Enzymatic synthesis of folylpolyglutamates: Characterization of the reaction and its products. J. Biol. Chem 1980;255:5776–5788. [PubMed: 6892914]
21. McClure WR, Chow Y. The kinetics and processivity of nucleic acid polymerases. Methods Enzymol 1980;64:277–297. [PubMed: 6990186]
22. Capson TL, Peliska JA, Kaboord BF, Frey MW, Lively C, Dahlberg M, Benkovic SJ. Kinetic characterization of the polymerase and exonuclease activities of the gene 43 protein of bacteriophage T4. Biochemistry 1992;31:10984–10994. [PubMed: 1332748]
23. Yuan Y, Barrett D, Zhang Y, Kahne D, Sliz P, Walker S. Crystal structure of a peptidoglycan glycosyltransferase suggests a model for processive glycan chain synthesis. Proc. Natl. Acad. Sci. U. S. A 2007;104:5348–5353. [PubMed: 17360321]
24. Barrett D, Wang TA, Yuan Y, Zhang Y, Kahne D, Walker S. Analysis of glycan polymers produced by peptidoglycan glycosyltransferases. J. Biol. Chem 2007;287:31964–31971. [PubMed: 17704540]
25. Shane B. Pteroylpoly(γ-glutamate) synthesis by *Corynebacterium* species: Studies on the mechanism of folylpoly(γ-glutamate) synthetase. J. Biol. Chem 1980;255:5663–5667. [PubMed: 6892913]
26. Bognar AL, Shane B. Purification and properties of *Lactobacillus casei* folylpoly-γ-glutamate synthetase. J. Biol. Chem 1983;258:12574–12581. [PubMed: 6138353]
27. Cichowicz DJ, Shane B. Mammalian folylpoly-γ-glutamate synthetase. Substrate specificity and kinetic properties. Biochemistry 1987;26:513–521. [PubMed: 3828321]
28. Tomsho JW, McGuire JJ, Coward JK. Synthesis and biological evaluation of (6*S*)- and (6*R*)-5,10-dideaza-5,6,7,8-tetrahydropteroyl poly-γ-glutamates as substrates for human folylpoly-γ-glutamate synthetase. Org. Biomol. Chem 2005;3:3388–3398. [PubMed: 16132101]
29. Rose IA. The isotope trapping method: Desorption rates of productive E-S complexes. Methods Enzymol 1980;64:47–59. [PubMed: 7374457]
30. Rose IA. Partition analysis: Detecting enzyme reaction cycle intermediates. Methods Enzymol 1995;249:315–340. [PubMed: 7791617]
31. Moran RG, Baldwin SW, Taylor EC, Shih C. The 6*S*-diastereomer and 6*R*-diastereomer of 5,10-dideaza-5,6,7,8-tetrahydrofolate are equiactive inhibitors of *de novo* purine synthesis. J. Biol. Chem 1989;264:21047–21051. [PubMed: 2592365]
32. Chen L, Qi H, Korenberg J, Garrow TA, Choi YJ, Shane B. Purification and properties of human cytosolic folylpoly-γ-glutamate synthetase and organization, localization, and differential splicing of its gene. J. Biol. Chem 1996;271:13077–13087. [PubMed: 8662720]
33. Gangjee A, Yu J, Kisliuk RL, Haile WH, Sobrero G, McGuire JJ. Design, synthesis, and biological activities of classical N-[4-[2-(2-amino-4-ethylpyrrolo[2,3-d]pyrimidin-5-yl)ethyl]benzoyl]-L-glutamic acid and its 6-methyl derivative as potential dual inhibitors of thymidylate synthetase and dihydrofolate reductase and as potential antitumor agents. J. Med. Chem 2003;46:591–600. [PubMed: 12570380]
34. Bradford MM. Rapid and sensitive method for quantitation of microgram quantities of protein utilizing principle of protein-dye binding. Anal. Biochem 1976;72:248–254. [PubMed: 942051]
35. Kuzmic P. Analysis and simulation of chemical kinetic, biochemical kinetic, and pharmacokinetic data. Anal. Biochem 1996;237:260–273. [PubMed: 8660575]
36. Segel, IH. Enzyme Kinetics. John Wiley & Sons; New York: 1975.
37. Moran RG, Colman PD, A FR, Rosowsky A. A mechanism for the addition of multiple moles of glutamate by folylpolyglutamate synthetase. J. Med. Chem 1984;27:1263–1267. [PubMed: 6148421]
38. Tomsho, JW. Ph.D. Thesis. University of Michigan; Ann Arbor: 2005. Folylpoly-γ-glutamate Synthetase: Kinetics of Multiple Glutamate Ligations.
39. Chen X-Y, Berti PJ, Schramm VJ. Ricin A-chain: Kinetic isotope effects and transition state structure with stem-loop RNA. J. Am. Chem. Soc 2000;122:1609–1617.
40. Tan X-J, Carlson HA. Docking studies and ligand recognition in folylpolyglutamate synthetase. J. Med. Chem 2005;48:7764–7772. [PubMed: 16302815]
41. Sun X, Cross JA, Bognar AL, Baker EN, Smith CA. Folate-binding triggers the activation of folylpolyglutamate synthetase. J. Mol. Biol 2001;310:1067–1078. [PubMed: 11501996]

42. Mathieu M, Debousker G, Vincent S, Viviani F, Bamas-Jacques N, Mikol V. *Escherichia coli* FolC structure reveals an unexpected dihydrofolate binding site providing an attractive target for anti-microbial therapy. J. Biol. Chem 2005;280:18916–18922. [PubMed: 15705579]

43. Sheng Y, Nurussaba K, Tsaksis Y, Shi X, Lu Q, Bognar AL. Mutagenesis of folylpolyglutamate synthetase indicates that dihydropteroate and tetrahydrofolate bind to the same site. Biochemistry 2008;47:2388–2396. [PubMed: 18232714]

44. Pai CH, Chiang BY, Ko TP, Chou CC, Chong CM, Yen FJ, Chen S, Coward JK, Wang HJ, Lin CH. Dual binding sites for translocation catalysis by *Escherichia coli* glutathionylspermidine synthetase. EMBO J 2006;25:5970–5982. [PubMed: 17124497]

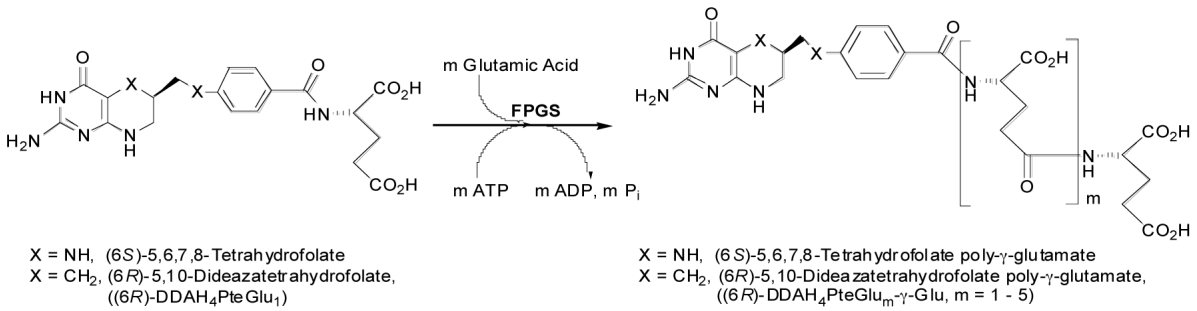

Figure 1.

The reaction catalyzed by FPGS. Note that the total number of glutamate residues added (m) is one less than the total number of glutamates in the product, $H_4PteGlu_n$; i.e., n = m +1.

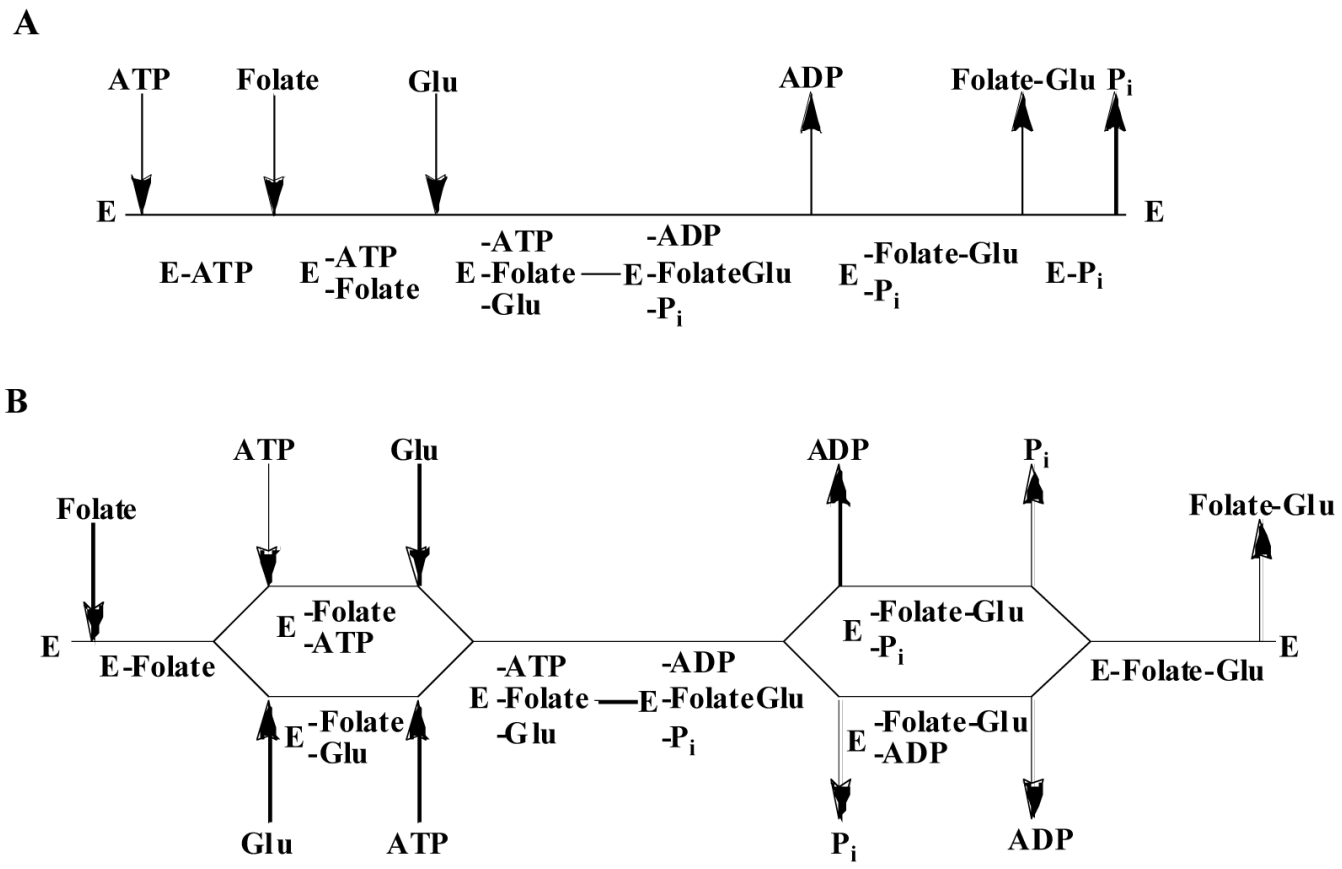

Figure 2.

A. The kinetic mechanism of FPGS as determined previously under non-processive ligation conditions. **B.** A possible kinetic mechanism that allows for processive glutamate ligations onto a single folate substrate. Any scheme in which the folate is the first substrate to bind and the folate-Glu product is the last to be released is compatible with a processive mechanism. A rearrangement step that places folate-Glu in the scheme in place of folate would be required for a processive mechanism. “Folate” is used as a generic term for the folate or antifolate substrate. “Folate-Glu” is also a generic term to denote the ligation product containing a single additional glutamate.

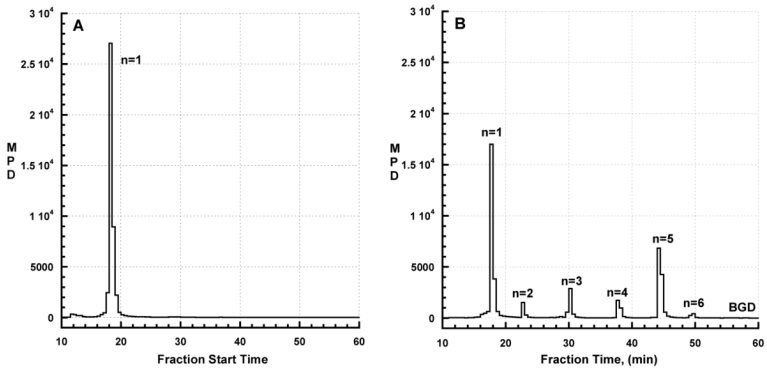

Figure 3.

Representative radiation chromatograms of the ion-pair HPLC method. **A.** Chromatogram of $DDAH_4Pte[^{14}C]Glu_1$ isolated from a FPGS-catalyzed reaction at t = 0 min. **B.** Chromatogram of biosynthetic $DDAH_4Pte[^{14}C]Glu_n$ isolated from a FPGS-catalyzed reaction of $DDAH_4Pte[^{14}C]Glu_1$ and L-glutamic acid to illustrate the separation of the various chain length polyglutamate products. BGD = background.

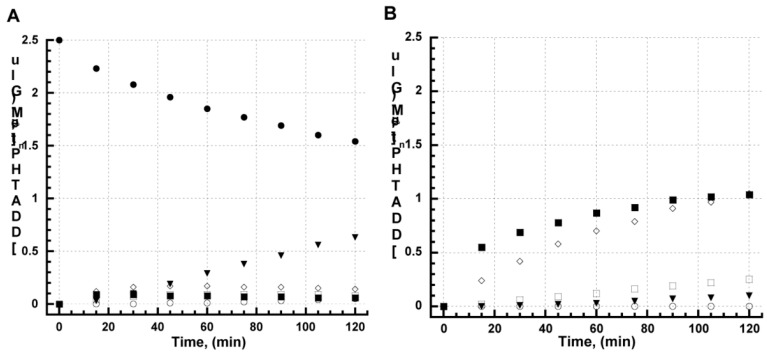

Figure 4.

Time course of the reaction of $DDAH_4Pte[^{14}C]Glu_1$ with partially purified hFPGS expressed in baculovirus-infected SF9 insect cells. The concentration of FPGS was approximately 14 nM. The concentrations of the glutamate and ATP substrates were saturating at 5 mM and 10 mM respectively. Product formation, $DDAH4PteGlu_n$,was analyzed as described in the Experimental Section and Supporting Information: n = 1 (□), n = 2 (□), n = 3 (◇), n = 4 (□), n = 5 (□), n = 6 (□). **A.** Reaction with 2.5 μM (~K_M) $DDAH_4Pte[^{14}C]Glu_1$. **B.** Reaction with 25 μM (~10 K_M) $DDAH_4Pte[^{14}C]Glu_1$. The data for n = 1 are not shown for clarity.

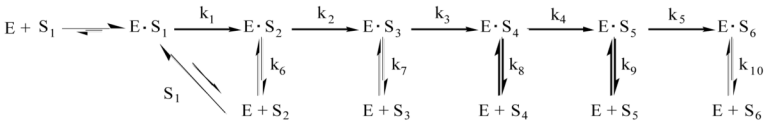

Figure 5.

Simplified kinetic scheme of the FPGS reaction. hFPGS is represented by E. $DDAH_4Pte[^{14}C]Glu_n$, n = 1-6, are represented by S_1, S_2, S_3, S_4, S_5, and S_6 respectively. The products of rate constants and enzyme-substrate complex concentrations, $k_1[E{\cdot}S_1] – k_5[E{\cdot}S_5]$, represent rates of ligation while $k_6[E{\cdot}S_2] – k_{10}[E{\cdot}S_6]$ represent rates of complex dissociation. The binding of ATP and glutamate and the release of P_i and ADP are excluded in this simplified scheme.

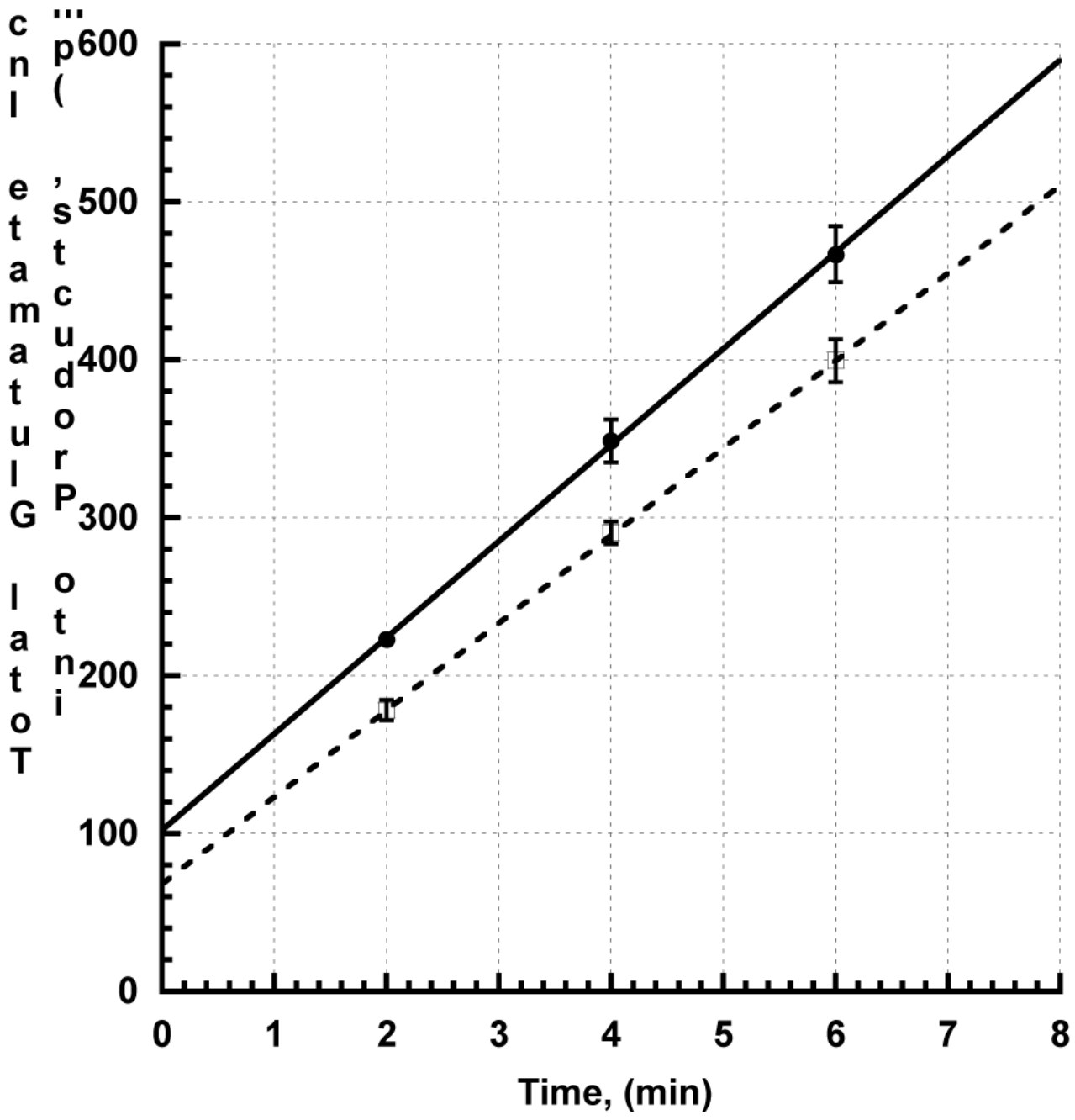

Figure 6.

Substrate trapping and control experiments (□) and (□) respectively. The concentration of hFPGS was 105 nM and $DDAH_4PteGlu_1$ was 25 μM. The average of three experiments was plotted with the error bars representing the standard deviation. When extrapolated to t = 0 min, 34.1 additional pmoles of glutamate were incorporated into product in the substrate trapping reaction when compared to the control reaction.

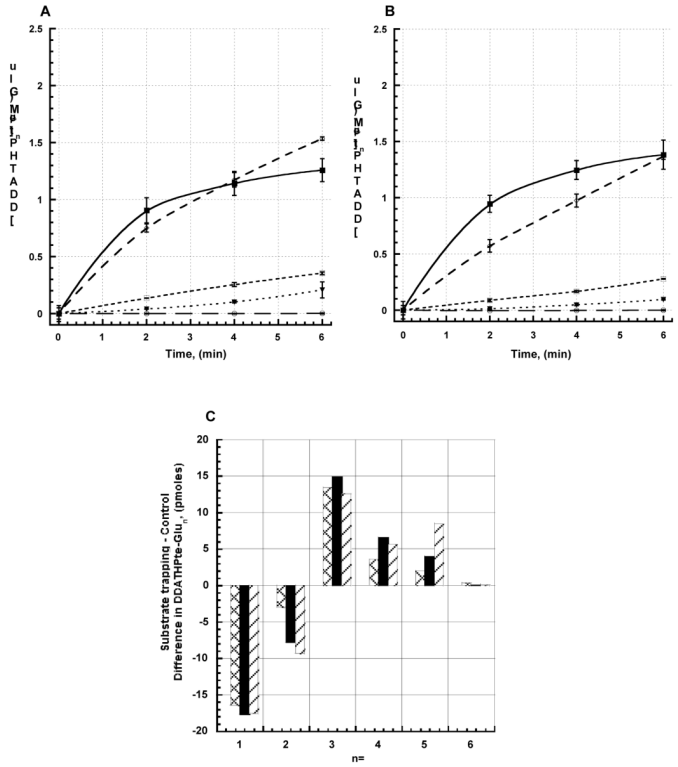

Figure 7.

Time dependence of $DDAH_4PteGlu_n$ formation. Biosynthetic DDAH4PteGlu$_n$,was analyzed as described in the Experimental Section and Supporting Information: n = 2 (□), n = 3 (◇), n = 4 (☐), n = 5 (☐), n = 6 (☐). The data for n = 1 are not shown in **A** or **B** for clarity. **A.** Product distribution under substrate trapping conditions (Figure 6, solid line). **B.** Product distribution under control conditions (Figure 6, dashed line). **C.** The difference in average product formation between the substrate trapping and control reactions by product chain length and time. At t = 0 min, there is no difference between the two reactions. t = 2 min (crossed), t = 4 min (solid), and t = 6 min (diagonal).

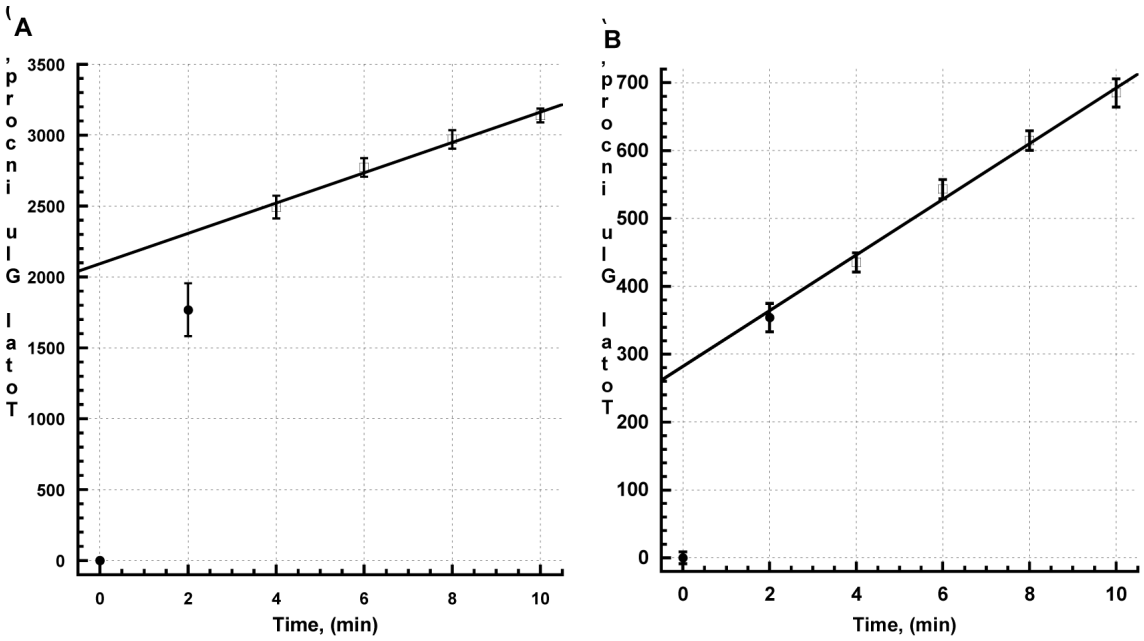

Figure 8.

Results of the pulse-chase experiments utilizing a pulse of 25 μM $DDAH_4$ Pte[^{14} C]Glu_1 in the presence of 80 pmoles hFPGS with a final concentration of 1.0 μM. **A.** Quench (□) or chase with 25 μM $DDAH_4PteGlu_1$ at t = 2 min followed by quenching at times indicated (□). **B.** Quench (□) or chase with 250 μM $DDAH_4PteGlu_1$ at t = 2 min followed by quenching at times indicated (□). The average of three experiments is plotted with the error bars representing the standard deviation. The difference in the value of the quench points between A and B arises from the experimental conditions, see Experimental, *Pulse-chase experiments*, 25 μM $DDAH_4PteGlu_1$ chase and 250 μM $DDAH_4PteGlu_1$ chase, respectively. The 25 μM $DDAH_4PteGlu_1$ chase experiment (**A**) utilized a 10-fold greater concentration, but equimolar amount, of hFPGS in the pulse than was used in the 250 μM $DDAH_4PteGlu_1$ chase experiment (**B**). The final concentration of hFPGS was identical during the chase phase in both experiments.